nature nanotechnology

Article

https://doi.org/10.1038/s41565-025-01982-5

An information ratchet improves selectivity in molecular recognition under non-equilibrium conditions

Received: 7 October 2024

Accepted: 25 June 2025

Published online: 01 August 2025



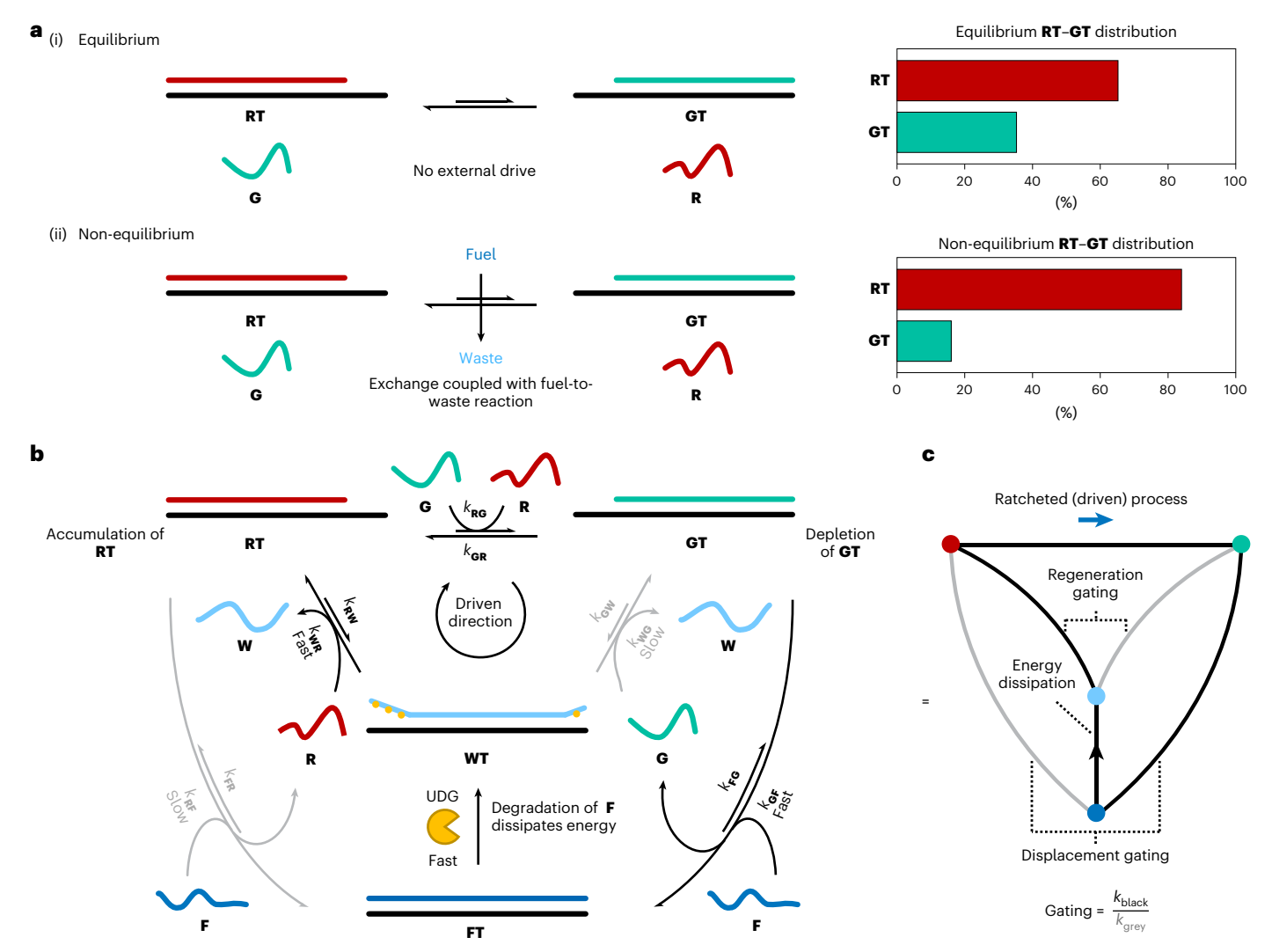
Benjamin M. W. Roberts **1**⁰, Erica Del Grosso **2**^{2,4}, Emanuele Penocchio **3**, Francesco Ricci **2** & Leonard J. Prins **1**

Molecular recognition is essential for controlling chemical processes, passing molecular instructions to elicit responses including structure formation, signalling and replication. Usually, the selectivity of molecular recognition is under thermodynamic control; however, when a higher fidelity is required, nature improves recognition selectivity by an error correction mechanism under an energy-dissipating kinetic-control regime. Here, exploiting DNA hybridization as a model, we present an abiotic example of an information ratchet mechanism that increases selectivity for the 'correct' duplex from 2:1 at equilibrium to 6:1 under energy-dissipating conditions. Structural asymmetry in the DNA strands introduces kinetic asymmetry in the reaction network, enabling enrichment under non-equilibrium conditions. We quantify the free-energy cost associated with enhanced selectivity using Shannon entropy formalism, finding that an increase in information of 0.33 bits is associated with at least 3.0 kJ mol⁻¹ of free energy. Moreover, the minimalistic structures of our error reduction system demonstrates that biomachinery is not necessary to increase molecular recognition fidelities above the thermodynamically expected values, thereby pointing a way towards solving Eigen's paradox.

Molecular recognition enables control over chemical processes at the molecular level. Recognition allows messages encoded in molecules to be transmitted, thereby relaying information and dictating a chemical response. This is most strikingly exemplified by deoxyribonucleic acid (DNA) in which information stored in the polynucleotide sequence of the double helix $^{1-3}$ is accessed by the molecular recognition of nucleobases. Yet, for processes in which the genetic information is used, molecular recognition based on thermodynamic selectivity alone is not sufficient for life to be viable $^{4-7}$. The error rate for equilibrium-controlled nucleobase recognition (about 1 in 1,000 for DNA strand extension) is too high and would result in the sequence degrading into unreadable noise after a few rounds of replication $^{6-7}$. Instead, biomolecular

machines such as DNA polymerase also perform error correction by kinetic proofreading 9 , thereby reducing the error rate in DNA replication by up to seven orders of magnitude to $1 \, \text{in} \, 10^{10}$ (refs. 4,9–11). This mechanism allows for the sequence-specific synthesis of a complementary DNA strand (or similarly, a ribonucleic acid strand or peptide), with a higher fidelity than could be achieved with thermodynamics-based selectivity 9,12,13 . The higher selectivity must come at the expense of energy consumption, as work is needed to reduce the system's entropy beyond thermodynamic equilibrium. Therefore, kinetic proofreading functions as a Brownian information ratchet mechanism $^{12-14}$, a mechanism in which the mediation of energy dissipation enables endergonic processes through the introduction of kinetic selection.

¹Department of Chemical Sciences, University of Padua, Padua, Italy. ²Department of Chemical Sciences and Technologies, University of Rome Tor Vergata, Rome, Italy. ³Department of Chemistry, Northwestern University, Evanston, IL, USA. ⁴These authors contributed equally: Benjamin M. W. Roberts, Erica Del Grosso. ⊠e-mail: francesco.ricci@uniroma2.it; leonard.prins@unipd.it



 $\label{eq:Fig.1} \textbf{Kinetic selectivity with an information ratchet. a}, \textit{Coupling energy dissipation from a fuel-to-waste reaction (vertical fuel-to-waste arrow) can drive DNA duplex exchange away from equilibrium, increasing the proportion of the red$ **RT**duplex.**b,c**, The chemical reaction network (**b**) and a simplified graph representation of the network (**c**), in which nodes represent the duplexes of**T**, transitions (reactions) are shown by solid lines and the fuel-to-waste reaction is indicated with an arrow, showing the direction in which energy is dissipated.**RT**and**GT** $duplexes can exchange via toehold-mediated strand displacement reactions 45,46 with free$ **G**and**R**, respectively, with the equilibrium slightly

favouring **RT**. Both **R** and **G** are displaced from **T** by **F**, although there is a kinetic preference to displace **G** more rapidly. The enzyme UDG converts **FT** into **WT**, weakening the association with **T** by removing uracil residues from the **F** strand 43 . **W** is then preferentially displaced by **R** or **G**, with a kinetic bias towards faster reaction with **R** due to a larger toehold. The black transitions show the kinetically preferred pathway for the reaction network (kinetic asymmetry), which couples energy dissipation with a ratcheted or driven process to drive it away from equilibrium.

An information ratchet refers to any system in which kinetic discrimination between the rates of formation and depletion of species within a reaction network is used to rectify the direction of a stochastic process (for example, a chemical equilibrium consisting of a forward reaction and its microscopic reverse). Performing kinetic selection enables an information ratchet to transduce free energy from external energy dissipation (for example, an exergonic fuel-to-waste reaction)¹⁵ to bias the rates of opposing forward and backward processes (Fig. 1a)^{12-14,16-19}. This can result in effects such as directional movement or the creation of non-equilibrium concentration distributions. The kinetic selection between the rates of reaction results in a kinetically preferred cyclic pathway within a non-equilibrium interconnected network of chemical reactions (Fig. 1b,c, black transitions)^{12-14,16-19}. The kinetic asymmetry¹⁷⁻²⁰ between forward and backward cycles ensures that the forward component of the driven process occurs more frequently than the backward component, driving it away from equilibrium and dissipating energy from an external source^{12,14}. It should be noted that the 'information' in the phrase 'information ratchet' is not strictly linked with the physical concept of information from Shannon's information theory 21 , but instead refers to the state-dependent reactivity of these systems, as if they have knowledge of their position within a reaction network 13,14 .

Apart from copying and translating DNA, information ratchet mechanisms are widely used in nature to control all kinds of process in which thermodynamic control is inadequate¹². Notable examples include performing directional movement with motor proteins, pumping concentration gradients, performing energy-demanding synthesis and constructing active structures such as microtubules^{12–14,22}. Perhaps owing to the complexity of designing such systems, Brownian ratchets are yet to find widespread applications in an abiotic context and remain largely confined to molecular machines^{13,14,23,24}. Only recently has the concept been extended to cover the energy-driven synthesis of materials and molecules^{20,25–29} and, more generally has awareness grown that ratchet mechanisms may be useful in many other areas^{12,14}. The transition towards non-equilibrium chemistry is expected to lead to

synthetic active matter with life-like properties $^{6,20,22,30-32}$. However, this transition requires the capacity to design information ratchets without using pre-existing biomolecular machines—in essence, the capacity to build a reaction network from scratch that dissipates energy to drive a chemical system away from equilibrium.

Error correction strategies that work via an information ratchet such as Hopfield kinetic proofreading³³ allow the sequence fidelity of a copy or translation product to be improved to such a level that a complex living organism can be sustained 9,12,34. This explains why evolution has found it to be worth paying the energetic cost of such a strategy. However, it has proved to be a markedly difficult feat to replicate in artificial systems^{35,36}. A recent key paper reported an artificial proofreading system that uses kinetic control to achieve error correction and bias the formation of a specific DNA duplex out of a set of possible products^{37,38}. The work elegantly replicates the scheme for kinetic proofreading as proposed in ref. 33, relying only on short DNA strands for kinetic discrimination, proving the feasibility of this network topology for performing error correction without enzymatic intervention. Unlike in biological systems, the process is driven by energy supplied by the formation of thermodynamically stable DNA duplexes, rather than by an exergonic chemical fuel-to-waste reaction³⁹.

Here we demonstrate that an information ratchet that improves selectivity in molecular recognition can be designed into a minimal chemical reaction network with a non-Hopfield topology. The system transduces free energy from a fuel-to-waste reaction^{15,40} to achieve enhanced selectivity during competitive DNA hybridization (Fig. 1a)41. The result is a selectivity that is dictated not only by the thermodynamics of binding but also by kinetic asymmetry in the reaction network (Fig. 1b,c)^{16,18,20,42}. Although energy dissipation is mediated by an enzyme-catalysed reaction⁴³, kinetic control in the reaction network is introduced through the structural features of the DNA strands themselves, rather than relying on 'black box' biochemical kinetic selectivity arising from an evolved biomolecular machine44. This demonstrates that kinetic selection processes can result from the intrinsic structures and reactivities of interacting molecules, through an information ratchet mechanism. The ability to design an information ratchet in an abiotic reaction network with non-Hopfield topology suggests that ratchet mechanisms have general applicability to perform error correction in molecular recognition processes in both abiotic and biotic contexts. Furthermore, we hypothesize that ratchet mechanisms are both necessary and sufficient to perform general error correction tasks.

Design of the DNA reaction network

The system, shown in Fig. 1, is based on the equilibrium between two strongly bound DNA duplexes RT and GT (that is, association constants of >10⁹ M⁻¹; Fig. 2a). These duplexes comprise the same template strand (T) and a complementary partner strand, either R (tagged with a red pentamethylene cyanine fluorophore at the 5' end and black hole quencher (BHQ) 2 at the 3' end) or G (tagged with a green fluorescein fluorophore at the 5' end and BHQ1 at the 3' end). Duplex formation increases the distance between the fluorophore and quencher, resulting in enhanced fluorescence intensity (indicated as red for RT and green for GT), which can, thus, be used as a measure for the concentrations of RT and GT duplexes (Fig. 2a). The strands R and G cannot bind T simultaneously as they compete for the central section of **T**. Duplex exchange $(\mathbf{RT} + \mathbf{G} \rightleftharpoons \mathbf{GT} + \mathbf{R})$ is efficient because of the presence of overhanging toeholds of four unpaired nucleobase residues at opposite ends of T (at the 5' end for RT and at the 3' end for GT), which expedite exchange via a toehold-mediated strand displacement reaction⁴⁵⁻⁴⁷ (Fig. 2b and Supplementary Section 4.4). At equilibrium, RT is slightly thermodynamically favoured over GT (equilibrium constant for displacement of **G** by \mathbf{R} , $K_{GR} = 3.47$; Fig. 2b and Supplementary Section 3.3).

The addition of 'fuel' strand, **F**, which is complementary to the full length of **T**, results in the formation of the **FT** duplex by displacing **R** or **G** with equilibrium constants of $K_{\text{RF}} = \frac{k_{\text{RF}}}{k_{\text{FR}}} = 13.1$ and $K_{\text{GF}} = \frac{k_{\text{GF}}}{k_{\text{FG}}} = 45.3$,

respectively (Supplementary Section 3.4). An enzyme, uracil-DNA glycosylase (UDG), hydrolyses deoxyuridine residues, which are present on the 3′ and 5′ ends of the **F** strand only, leading to the formation of abasic sites (Fig. 2c)⁴³. This chemical modification transforms **F** into a waste strand, **W**, with a substantially lower affinity for **T** (equilibrium constant for the displacement of **W** by **F**, K_{WF} = 5.80 × 10⁴; Supplementary Sections 3.4 and 3.5). Uracil deletion results in the destabilization of the 3′ and 5′ ends of the **WT** duplex, enabling an expedited displacement of **W** by free **R** (K_{WR} = $\frac{k_{WR}}{k_{RW}}$ = 4.44 × 10³) or **G** (K_{WG} = $\frac{k_{WC}}{k_{GW}}$ = 1.28 × 10³; Supplementary Section 3.5), closing the reaction cycle and repopulating **RT** and **GT**. The hydrolysis of deoxyuridine is exergonic and provides the free energy that drives the cycle^{14,15}. The system is explicitly designed as an information ratchet, containing the required stochastic process (**RT** + **G** \rightleftharpoons **GT** + **R**), which is incorporated into two catalytic cycles for converting **F** to **W**, such that a kinetic preference for once cycle (kinetic asymmetry) rectifies the direction of the stochastic process and creates bias ^{12,14,42}.

Stepwise operation kinetics

An information ratchet mechanism requires the presence of kinetic asymmetry in the chemical reaction network (Fig. 1, black versus grey reaction arrows; Supplementary Section 4.8)^{16,18,20}. Kinetic parameters for all the relevant processes were obtained by operating the system in a stepwise manner (Fig. 3), in the first instance, by adding F to pre-formed duplexes of either RT or GT (blue area, hollow circles) followed by the addition of UDG (yellow area, hollow circles). These experiments can be fitted to a kinetic model to show that F reacts faster with GT than RT $(\frac{k_{GF}}{k_{DF}} = 3.46$; Fig. 3 (blue area) and Supplementary Section 4.5), but that **WT** reacts faster with **R** than **G** ($\frac{k_{\text{WR}}}{k_{\text{WG}}}$ = 125; Figs. 2c and 3 (yellow area) and Supplementary Section 4.6). These ratios of rates are known as the chemical gating of the respective displacement and regeneration steps and quantify the kinetic bias in the cycle (Supplementary Section 4.8)^{14,16}. The similarity of the displacement gating and equilibrium constant quantifying the thermodynamic preference for **GT** over **RT** ($K_{GR} = 3.47$) indicates that these two factors may be governed by the same interactions. Although possibly coincidental, this matches other situations in which the introduction of a thermodynamic preference (power stroke) is directly compensated by the chemical gating in information ratchets 16,48. Conversely, the much larger regeneration gating, which is the main source of kinetic asymmetry in the system, is the result of the much lower stability of the WT duplex in the R-binding to ehold region caused by the UDG-mediated removal⁴³ of three-base-pair interactions compared with just one in the **G**-binding toehold region.

Having determined the kinetic parameters in the isolated **R/G** experiments, next, the experiment was repeated in the presence of both RT and GT in equimolar amounts (that is, R and G are not in competition for binding to T; Fig. 3b (solid circles)). Under these conditions, the kinetic bias establishes a reaction current (circular arrow, Fig. 3a (third panel)), where W is first displaced from WT by R, after which R is then displaced from RT by G to allow RT and GT to re-equilibrate more rapidly. This new pathway for the repopulation of **GT**, which has become accessible because of the presence of **R** in the system, is much faster than the direct displacement of WT by free G, as evidenced by the much faster increase in GT concentration under these conditions (Fig. 3b). This shows that the chemical reaction network is under kinetic control and meets the required characteristics for an information ratchet mechanism, enabling it to rectify stochastic RT-GT exchange by control over kinetic biases in a chemical reaction network^{12-14,16-18}. For this system, this implies that the energy released from F-to-W conversion is used to drive the **RT/GT** ratio to a non-equilibrium value ^{12,15}.

Continuous operation kinetics

To observe non-equilibrium behaviour (and to differentiate the system from a simple kinetically controlled reaction that progresses towards

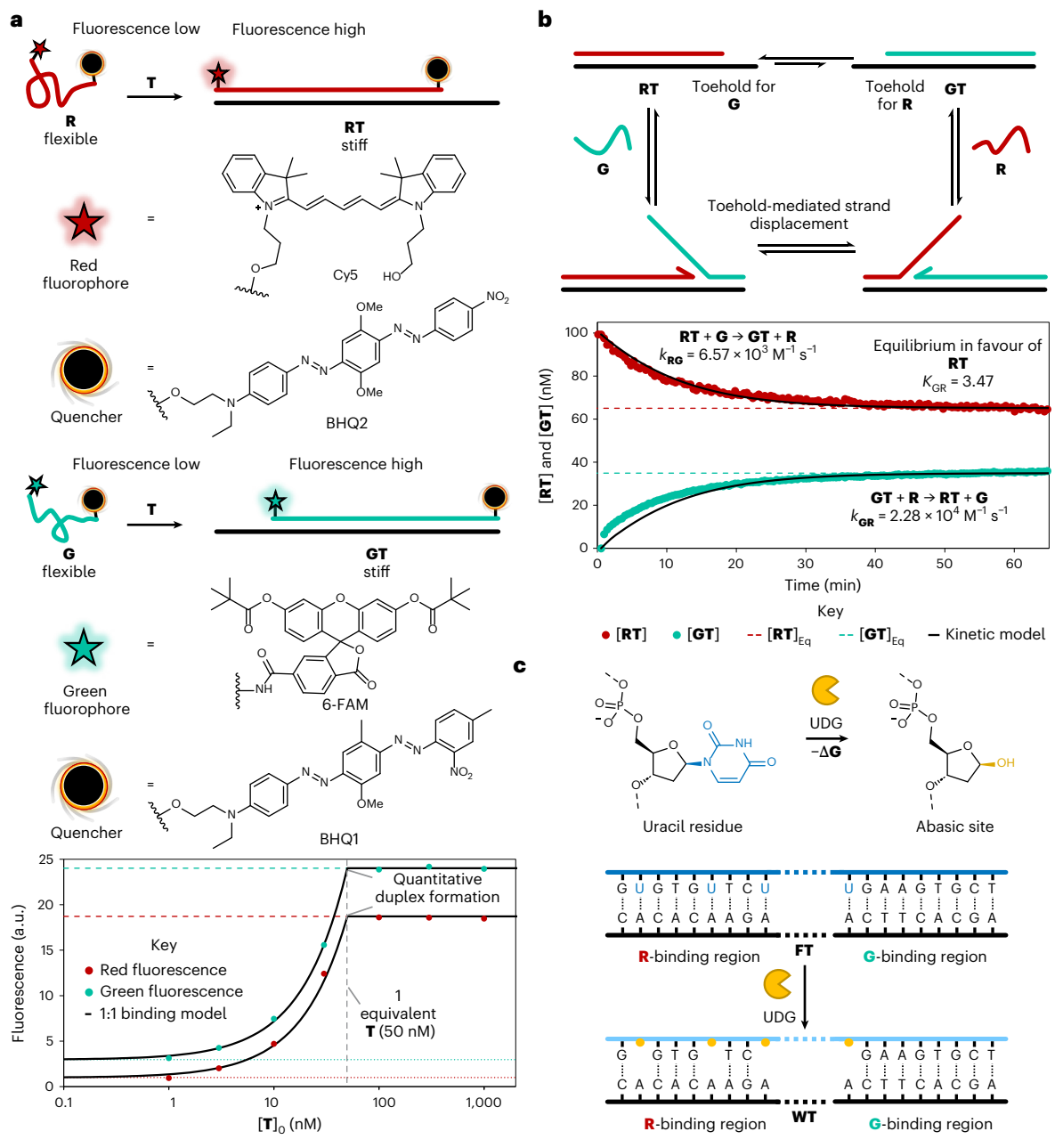
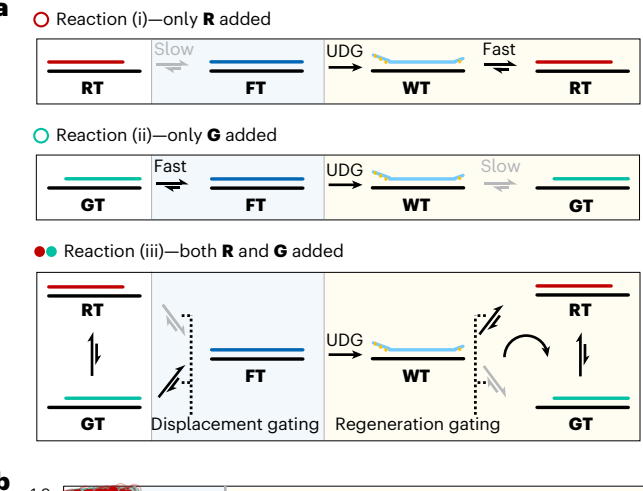


Fig. 2 | **Mechanisms for the key steps. a**, **R** and **G** strands are tagged with a fluorophore at one end and an absorption-matched BHQ at the other. The free strands are flexible, tending to bring the fluorophore and quencher into close proximity, thereby reducing their fluorescence. The duplexes **RT** and **GT** are stiffer due to hybridization, moving the fluorophore further from the quencher, thereby increasing their fluorescence. Hence, fluorescence can be used to measure the concentration of the duplex, as can be seen from the graph, showing the titration of **T** into **R** or **G** (50 nM). **b**, Mechanism for toehold-mediated strand displacement ^{45,46}. **R** and **G** are shorter than **T**, leaving toehold regions in **RT**

and **GT**. Free strands can bind the toehold and progressively unzip the other strand, rather than requiring full dissociation for exchange to occur. Addition of **R** (100 nM) into **GT** (100 nM) results in a rate of exchange faster than can be explained by dissociation. **c**, Creation of the asymmetric labile regions at the 5′ and 3′ ends of the **WT** duplex. The enzyme UDG selectively removes uracil residues via an exergonic hydrolysis 43 . The **G**-binding region contains only one uracil so only a single unbound adenine residue is formed by UDG for **G** to bind. Conversely, the **R**-binding region contains three uracil residues, resulting in a much more destabilized section to expedite the displacement of **W** by **R**.

a thermodynamically stable product) 12, the reaction should be performed in conditions where ${\bf R}$ and ${\bf G}$ compete for binding to ${\bf T}$ and where the full cycle can be completed 15. This effectively establishes a catalytic cycle 16,49, in which kinetic biases (chemical gatings) couple ${\bf F}$ -to- ${\bf W}$ conversion with ${\bf G}{\bf T}$ depletion and ${\bf R}{\bf T}$ formation (Fig. 1 and Supplementary Section 4.8). These conditions are achieved by adding ${\bf F}$ directly into a pre-equilibrated reaction mixture containing UDG with an excess of ${\bf R}$ and ${\bf G}$ compared with ${\bf T}$ (Fig. 4a). When ${\bf F}$ was added under these conditions (yellow area), the kinetic asymmetry in the reaction network

led to a preferential depletion of **GT**, whereas **RT** was preferentially regenerated (Supplementary Section 4.7). To see **RT** accumulation, it is important that a sufficient concentration of UDG is present so that the fuel-to-waste reaction is faster than **RT**-to-**GT** equilibration 14,50 . The kinetic model fitted on the data from the stepwise experiments (Figs. 2 and 3) closely matched the observed data (Fig. 4b, black lines), showing that the behaviour is consistent with the proposed mechanism $^{12-14,16-18}$. The model indicates that UDG is not selective for the **FT** duplex, resulting in high background fuel decomposition, but this has no further



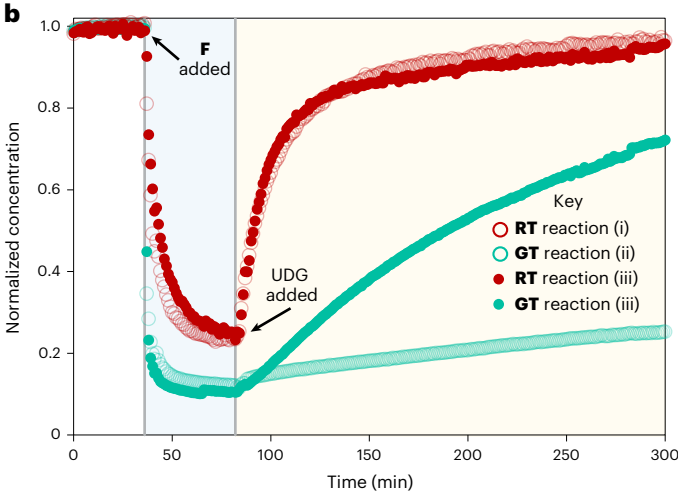


Fig. 3 | Stepwise investigation of the reaction parameters. a, Schematics showing the two sets of reactions with either **R** or **G** and with both **R** and **G**. In the latter case, a pathway is established that enables the more rapid regeneration of **GT** by bypassing the slow step in which **G** directly displaces **W**. **b**, Normalized concentrations of the fluorescent duplexes as, first, 1 equivalent of **F** (blue background); then, UDG (yellow background) is added. The hollow circles represent the reactions with only one fluorescent strand present: red shows reaction (i) with only **R** (100 nM of **R** and **T**, then 100 nM of **F** and then 20 U ml⁻¹ of UDG) and green shows reaction (ii) with only **G** (100 nM of **G** and **T**, then 100 nM of **F** and then 20 U ml⁻¹ of UDG). The filled circles show reaction (iii) with 0.5 equivalents each of **R** and **G** (50 nM of **R** and **G**, 100 nM of **T**, 100 nM of **F** and then 20 U ml⁻¹ of UDG). The presence of **R** increases the rate of **GT** regeneration by approximately an order of magnitude, whereas the rate of **RT** regeneration is unaffected.

implications for the design strategy beyond poor efficiency of this precise system and has no effect on the non-equilibrium **RT/GT** ratio⁵¹.

The operation resulted in an increased **RT/GT** ratio from around 2:1 (30% excess) at equilibrium (Fig. 4c,e(ii)); the expected ratio with $K_{RG} = 3.47$ with 50 nM each of **R**, **G** and **T**), reaching a peak of 5:1 (65% excess) under the non-equilibrium conditions (Fig. 4c,e(iii)) with 4 equivalents of **F**, and up to 6:1 (71% excess) with 10 equivalents (Supplementary Sections 4.7 and 6.3). This is the primary evidence that energy consumption drives the system away from equilibrium. Importantly, the elevated ratio is the result of kinetic selectivity enhancing molecular recognition and not a thermodynamically controlled response to a transient stimulus ^{15,22,41}. Usually, in transiently responsive cases, the responsive reaction remains in equilibrium at all times, while the equilibrium position of the responsive reaction is shifted by a stimulus (for example, pH), which is itself changing over time ^{47,50}. By contrast, here the elevated **RT/GT** ratio long outlasts the presence of the fuel, **F**,

showing that the reaction system is under kinetic control and sustained by a reaction current ($WT \rightarrow RT \rightarrow GT$) rather than equilibrated to the concentration of **F**. Remarkably, the absolute concentration of **RT** even increases above the equilibrium value before slowly re-equilibrating (Fig. 4b and Supplementary Section 4.7). This behaviour is not possible for a responsive system equilibrating to a transient stimulus as it requires that the non-equilibrium free-energy contribution from these species increases at some point during the reaction (Supplementary Section 6.2). This demonstrates that the information ratchet mechanism in this system stores some of the free energy transduced from the fuel-to-waste decomposition by keeping concentrations of **RT** and **GT** away from equilibrium 20,52 .

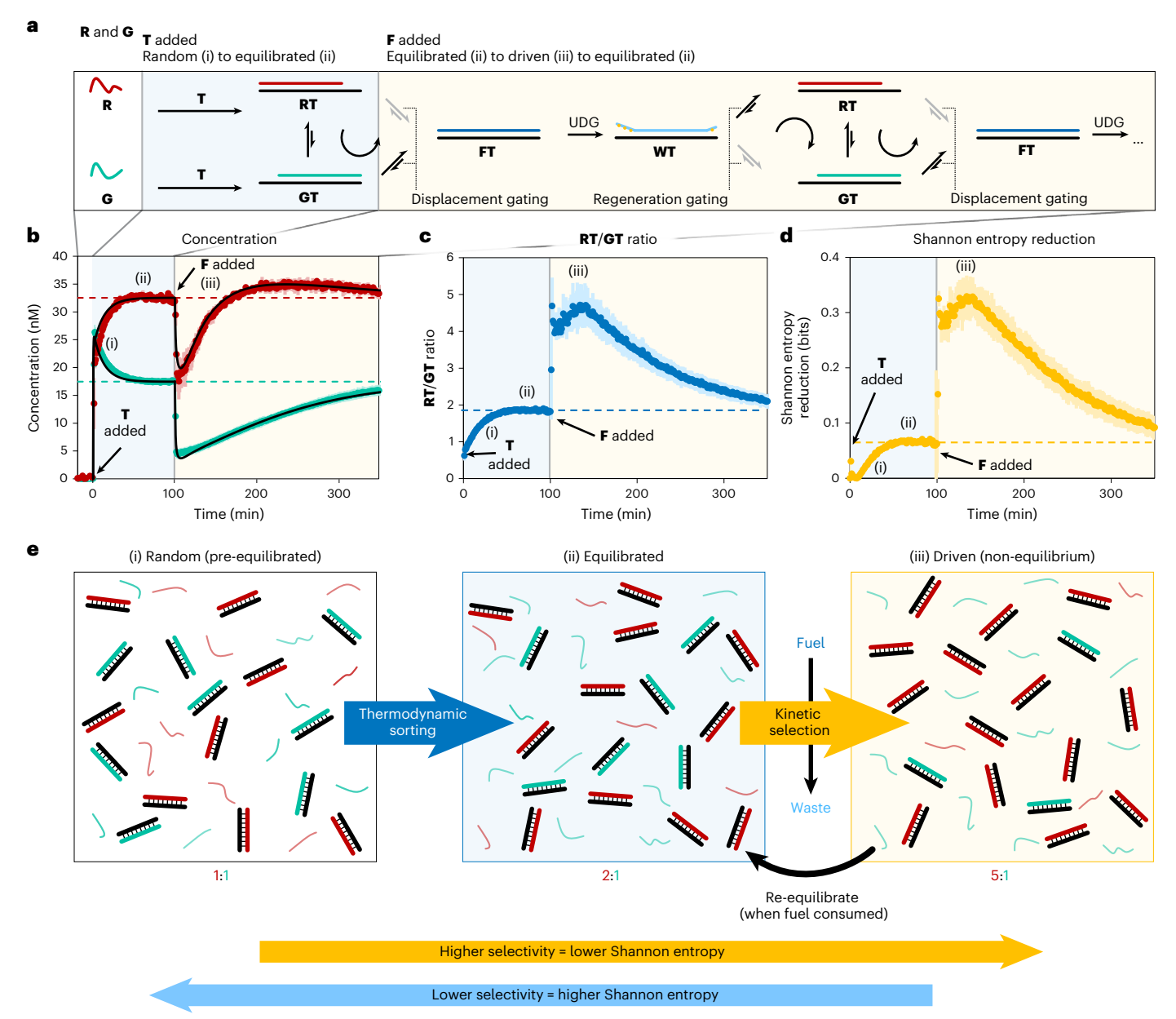
The attribution of enhanced selectivity to transient effects could be effectively ruled out by operating under chemostatted conditions at which the fuel and waste concentrations in the system are kept constant as a result of a continuous exchange with the environment. Regrettably, experimental setups that permit the study of such 'open systems' remain underdeveloped ^{53,54}. Therefore, we performed simulations of our system under chemostatted conditions, exploiting the available kinetic parameters (Supplementary Section 7). The simulations confirm that the non-equilibrium composition is maintained at the steady state, effectively proving that the kinetic model is consistent with an information ratchet.

Quantifying free-energy storage and selectivity

A mark of success of an information ratchet is how effectively free energy can be transduced from the fuel-to-waste process to the driven variable. The free energy transduced by the information ratchet and stored in the **RT**–**GT** disequilibrium can be assessed through the contribution of the **RT** and **GT** duplexes and unbound **R** and **G** to the relative non-equilibrium system free energy (compared with equilibrium)^{48,52}. At its peak, the free energy stored in this disequilibrium is roughly equivalent to that of a hydrogen bond (0.15 mJ l⁻¹ \approx 3.0 kJ mol⁻¹ based on [**T**]₀ = 50 nM and [**F**]₀ = 500 nM; or 0.05 mJ l⁻¹ \approx 1.0 kJ mol⁻¹ based on [**T**]₀ = 50 nM and [**F**]₀ = 200 nM; Supplementary Sections 6.1 and 6.2). This suggests that the system is driven with enough power to potentially perform useful work, such as movement, formation of high-energy structures or error correction ^{12,40,48,49,55}.

The role of free-energy transduction that is of interest in the current case is the creation of an extra non-equilibrium bias in favour of **RT** over **GT**, which constitutes an error correction. The progress of the system can be tracked as it starts out from randomly assorted (Fig. 4b-e(i)) to equilibrated and slightly in favour of **RT** (Fig. 4b-e(ii)) and then driven away from equilibrium by the information ratchet to a higher bias in favour of **RT** (Fig. 4b-e(iii)). With each stage, an increase in selectivity towards **RT** reduces the uncertainty arising from imperfect molecular recognition about which the duplex is formed by each template strand. This reduction in uncertainty is conveniently quantified using Shannon entropy (Methods), a measure of the average level of uncertainty associated with a random variable (Fig. 4d). A reduction in Shannon entropy reflects the capacity of a molecular recognition event to alter the amount of information in a related output, for example, the colour of fluorescence, as the outcome is less uncertain⁵⁶. Therefore, it can be interpreted as a direct measure of the capacity of a molecular recognition event (for example, duplex formation) to relay a chemical signal or encoded instructions (for example, the wavelength of the fluorescence output). The analysis of selectivity in molecular recognition in terms of Shannon entropy has advantages over typical quantifications of selectivity such as binding constants or ratios since it is independent of concentration and can deal with systems that have multiple possible outcomes or where outcomes have cascading effects throughout a chemical reaction network.

Using an equilibrium approach (that is, without error correction; Fig. 4b-e, position (ii)), the Shannon entropy associated with molecular recognition can only be reduced by increasing the binding affinity of



 $\label{eq:Fisher} \textbf{Fig. 4} \ | \ In situ \ operation \ of the error-correcting \ information \ ratchet. \ First \ T \ (50 \ nM; blue \ area) \ and \ then \ F \ (200 \ nM; yellow \ area) \ were \ added to a mixture \ of \ R \ and \ G \ (each 50 \ nM) \ and \ UDG \ (1 \ U \ ml^{-1}). \ a_r \ Schematics \ to \ represent the \ reactions that occur. \ b_r \ Concentrations \ of \ RT \ and \ GT \ throughout the \ reaction. \ The dotted lines show the \ expected \ equilibrium \ values, \ and \ the \ solid \ black \ lines \ indicate \ the \ expected \ values \ based \ on \ the \ kinetic \ simulations. \ c_r \ RT/GT \ ratio \ observed \ at \ different \ time \ points. \ The \ equilibrium \ ratio \ (-2:1; \ dotted \ line) \ is \ reached \ after \ the \ addition \ of \ T \ (blue \ background). \ The \ addition \ of \ F \ (yellow)$

background) increases the bias towards \mathbf{RT} (-5:1). \mathbf{d} , Quantification of selectivity as Shannon entropy reduction of the \mathbf{RT} - \mathbf{GT} degree of freedom from a random pre-equilibrated mixture. At equilibrium, Shannon entropy is decreased by 0.07 bits by duplex formation (dotted line). As the bias towards \mathbf{RT} increases, Shannon entropy decreases further, reaching 0.35 bits. \mathbf{e} , Representations of the duplex distributions at three key points in the reaction ((i)–(iii), as indicated in the graphs). Data are presented as mean values for each time point across three independent replications \pm the standard deviation shown by the shaded error bars.

the 'correct' partner relative to the 'incorrect' partners^{48,52}. In other words, the 'binding free-energy' difference between the correct and incorrect duplexes must directly compensate for any Shannon entropy reduction (increased selectivity) of the system. The equilibrium strategy introduces structural restrictions (competitive binders must be sufficiently different to be recognized) as well as difficulties for creating dynamic systems (strong binding may result in slow dissociation rates, making exchange difficult and decrease responsiveness). Using an information ratchet to transduce free energy from an external source (fuel-to-waste reaction) provides an alternative source of energy dissipation to create bias towards **RT** (ref. 48), enabling molecular recognition to proceed with greater specificity (Fig. 4d,e(iii)). The

ratchet mechanism corrects the 'error' of **GT** formation by continuously converting it to **RT** via the forward-driven cycle (Fig. 1b).

Quantifying selectivity using physical quantities such as the stored free energy or Shannon entropy (Methods and Supplementary Section 6) allows a comparison between different systems with different numbers of possible products/outcomes (that is, binary selectivity in the current system versus quaternary selectivity in DNA nucleotide selection versus 21-fold selectivity in peptide selection (there are codons for 20 natural amino acids and a 'stop' function)), where a strict correct-to-incorrect ratio may be unhelpful. On the basis of the above analysis, the free-energy cost associated with the non-equilibrium enhanced selectivity in our system is at least 3.0 kJ mol⁻¹ (RT-GT free

energy per mol at the highest selectivity) for an increase in information of 0.33 bits (0.40 bits – 0.07 bits), and using 500 nM of **F**. Using 200 nM of **F**, an increase of 0.28 bits (0.35 bits – 0.07 bits) is associated with a free-energy cost of 0.92 kJ mol⁻¹.

Conclusions

We have shown that an information ratchet can enhance selectivity in molecular recognition by demonstrating a change in the template's preference for binding partners at the expense of free-energy consumption. Although our observation is limited to a relatively simple redistribution between two species, the results provide a conceptually new direction for improving chemical recognition processes in general. Although in chemical recognition research, the traditional focus is on the design of receptors with high thermodynamic affinity for one species out of a mixture ^{22,41}, our results suggest that chemical sensors that operate under non-equilibrium conditions applying an information ratchet mechanism may be more effective ⁵⁷. Moreover, our results extend the application of information ratchets from molecular machines and materials to the field of molecular recognition, reinforcing the insight that non-equilibrium systems rely on universal physical-chemical principles.

The transition from a conceptual demonstration to a practical application in the field of dissipative DNA nanotechnology⁴¹ requires several improvements. A major drawback is the high background rate of fuel consumption, which is not uncommon in synthetic non-equilibrium systems¹⁵. The most prominent solution would be to improve the 'catalytic efficiency' using fuels that are only activated when bound, so they are only consumed by the ratchet mechanism. A second drawback is the limited availability of technology that allows non-equilibrium chemical systems to be studied under steady-state conditions in which just fuel and waste are exchanged with the environment^{54,58}.

The importance of molecular recognition under non-equilibrium conditions is evident from nature's ubiquitous reliance on kinetic proofreading for nucleic and peptide synthesis $^{9-12}$, suggesting that operating under non-equilibrium conditions is of particular value when information must be read many times to synthesize multiple daughter DNA/ribonucleic acid strands or proteins, respectively. Kinetic control using an information ratchet can compensate for a lower thermodynamic preference 12 , which allows templates to be used catalytically, amplifying their information content 9,40,48,55,59 .

The most important difference of this system compared with protein biosynthesis or DNA replication is that the process reported here proceeds with no complex biological machinery involved in the error-correcting kinetic selection steps; the enzyme is not the source of kinetic asymmetry in the network. The UDG enzyme is only used in a non-selective step to create an activated WT adduct, which could plausibly be replaced with a non-biological process^{60,61}. Instead, the kinetic selectivity is encoded into the chemical reaction network in the structures of the short DNA sequences of the reacting species R, G, T and **F**, demonstrating that enhanced molecular recognition is plausible without invoking complex biomachinery44. This is of key interest in relation to Eigen's paradox: that error-correcting processes are needed to explain the origin of biomachines that perform error correction. These machines, which are needed for the high-fidelity DNA replication required for life to persist, are encoded in long genes that cannot be copied sufficiently accurately in the absence of the same structures. If the improved fidelity we have observed could be translated to a self-replicating read-write system, the ability to perform error correction with such small nucleic acid strands could provide a potential solution to Eigen's paradox^{6,7} and explain how chemistry could have spontaneously leapt from inactive to active matter.

Online content

Any methods, additional references, Nature Portfolio reporting summaries, source data, extended data, supplementary information,

acknowledgements, peer review information; details of author contributions and competing interests; and statements of data and code availability are available at https://doi.org/10.1038/s41565-025-01982-5.

References

- Watson, J. D. & Crick, F. H. C. Molecular structure of nucleic acids: a structure for deoxyribose nucleic acid. *Nature* 171, 737–738 (1953).
- Wilkins, M. H. F., Stokes, A. R. & Wilson, H. R. Molecular structure of nucleic acids: molecular structure of deoxypentose nucleic acids. *Nature* 171, 738–740 (1953).
- 3. Franklin, R. E. & Gosling, R. G. Molecular configuration in sodium thymonucleate. *Nature* **171**, 740–741 (1953).
- Song, Y. & Hyeon, C. Thermodynamic uncertainty relation to assess biological processes. J. Chem. Phys. 154, 130901 (2021).
- 5. Song, Y. & Hyeon, C. Thermodynamic cost, speed, fluctuations, and error reduction of biological copy machines. *J. Phys. Chem. Lett.* **11**, 3136–3143 (2020).
- 6. Adamski, P. et al. From self-replication to replicator systems en route to de novo life. *Nat. Rev. Chem.* **4**, 386–403 (2020).
- Eigen, M. Selforganization of matter and the evolution of biological macromolecules. *Naturwissenschaften* 58, 465–523 (1971).
- Goodman, M. F. Hydrogen bonding revisited: geometric selection as a principal determinant of DNA replication fidelity. *Proc. Natl Acad. Sci. USA* 94, 10493–10495 (1997).
- 9. Sartori, P. & Pigolotti, S. Thermodynamics of error correction. *Phys. Rev. X* **5**, 041039 (2015).
- Mallory, J. D., Kolomeisky, A. B. & Igoshin, O. A. Trade-offs between error, speed, noise, and energy dissipation in biological processes with proofreading. *J. Phys. Chem. B* 123, 4718–4725 (2019).
- Kunkel, T. A. & Bebenek, K. DNA replication fidelity. Annu. Rev. Biochem. 69, 497–529 (2000).
- Borsley, S., Gallagher, J. M., Leigh, D. A. & Roberts, B. M. W. Ratcheting synthesis. Nat. Rev. Chem. 8, 8–29 (2024).
- Sangchai, T., Al Shehimy, S., Penocchio, E. & Ragazzon, G. Artificial molecular ratchets: tools enabling endergonic processes. Angew. Chem. Int. Ed. 62, e202309501 (2023).
- Borsley, S., Leigh, D. A. & Roberts, B. M. W. Molecular ratchets and kinetic asymmetry: giving chemistry direction. *Angew. Chem. Int.* Ed. 63, e202400495 (2024).
- Borsley, S., Leigh, D. A. & Roberts, B. M. W. Chemical fuels for molecular machinery. Nat. Chem. 14, 728–738 (2022).
- Amano, S. et al. Using catalysis to drive chemistry away from equilibrium: relating kinetic asymmetry, power strokes, and the Curtin-Hammett principle in Brownian ratchets. J. Am. Chem. Soc. 144, 20153–20164 (2022).
- Astumian, R. D. Kinetic asymmetry and directionality of nonequilibrium molecular systems. *Angew. Chem. Int. Ed.* 63, e202306569 (2024).
- Astumian, R. D. Irrelevance of the power stroke for the directionality, stopping force, and optimal efficiency of chemically driven molecular machines. *Biophys. J.* 108, 291–303 (2015).
- Astumian, R. D. Kinetic asymmetry allows macromolecular catalysts to drive an information ratchet. *Nat. Commun.* 10, 3837 (2019).
- 20. Ragazzon, G. & Prins, L. J. Energy consumption in chemical fuel-driven self-assembly. *Nat. Nanotechnol.* **13**, 882–889 (2018).
- 21. Parrondo, J. M. R., Horowitz, J. M. & Sagawa, T. Thermodynamics of information. *Nat. Phys.* 11, 131–139 (2015).
- Das, K., Gabrielli, L. & Prins, L. J. Chemically fueled self-assembly in biology and chemistry. *Angew. Chem. Int. Ed.* 60, 20120–20143 (2021).

- Borsley, S., Kreidt, E., Leigh, D. A. & Roberts, B. M. W. Autonomous fuelled directional rotation about a covalent single bond. *Nature* 604, 80–85 (2022).
- Borsley, S., Leigh, D. A. & Roberts, B. M. W. A doubly kinetically-gated information ratchet autonomously driven by carbodiimide hydration. J. Am. Chem. Soc. 143, 4414–4420 (2021).
- Olivieri, E., Gallagher, J. M., Betts, A., Mrad, T. W. & Leigh, D. A. Endergonic synthesis driven by chemical fuelling. *Nat. Synth.* 3, 707–714 (2024).
- Al Shehimy, S. et al. Progressive endergonic synthesis of Diels-Alder adducts driven by chemical energy. Angew. Chem. Int. Ed. 63, e202411554 (2024).
- Marchetti, T., Frezzato, D., Gabrielli, L. & Prins, L. J. ATP drives the formation of a catalytic hydrazone through an energy ratchet mechanism. *Angew. Chem. Int. Ed.* 62, e202307530 (2023).
- Ota, E., Wang, H., Frye, N. L. & Knowles, R. R. A redox strategy for light-driven, out-of-equilibrium isomerizations and application to catalytic C-C bond cleavage reactions. *J. Am. Chem. Soc.* 141, 1457–1462 (2019).
- 29. Shin, N. Y., Ryss, J. M., Zhang, X., Miller, S. J. & Knowles, R. R. Light-driven deracemization enabled by excited-state electron transfer. *Science* **366**, 364–369 (2019).
- Rieß, B., Grötsch, R. K. & Boekhoven, J. The design of dissipative molecular assemblies driven by chemical reaction cycles. *Chem* 6, 552–578 (2020).
- Walther, A. & Giuseppone, N. Out-of-Equilibrium (Supra) Molecular Systems and Materials (Wiley-VCH, 2021).
- Merindol, R. & Walther, A. Materials learning from life: concepts for active, adaptive and autonomous molecular systems. *Chem.* Soc. Rev. 46, 5588–5619 (2017).
- Hopfield, J. J. Kinetic proofreading: a new mechanism for reducing errors in biosynthetic processes requiring high specificity. Proc. Natl Acad. Sci. USA 71, 4135–4139 (1974).
- Arias-Gonzalez, J. R. Entropy involved in fidelity of DNA deplication. PLoS ONE 7, e42272 (2012).
- Wochner, A., Attwater, J., Coulson, A. & Holliger, P. Ribozyme-catalyzed transcription of an active ribozyme. Science 332, 209–212 (2011).
- Attwater, J., Wochner, A. & Holliger, P. In-ice evolution of RNA polymerase ribozyme activity. Nat. Chem. 5, 1011–1018 (2013).
- Mukherjee, R., Sengar, A., Cabello-García, J. & Ouldridge, T. E. Kinetic proofreading can enhance specificity in a nonenzymatic DNA strand displacement network. J. Am. Chem. Soc. 146, 18916–18926 (2024).
- Cabello-Garcia, J., Mukherjee, R., Bae, W., Stan, G.-B. V. & Ouldridge, T. E. Information propagation through enzyme-free catalytic templating of DNA dimerization with weak product inhibition. *Nat. Chem.* https://doi.org/10.1038/s41557-025-01831-x (2025).
- Haley, N. E. C. et al. Design of hidden thermodynamic driving for non-equilibrium systems via mismatch elimination during DNA strand displacement. *Nat. Commun.* 11, 2562 (2020).
- Amano, S. et al. Insights from an information thermodynamics analysis of a synthetic molecular motor. *Nat. Chem.* 14, 530–537 (2022).
- 41. Del Grosso, E., Franco, E., Prins, L. J. & Ricci, F. Dissipative DNA nanotechnology. *Nat. Chem.* **14**, 600–613 (2022).
- Penocchio, E., Bachir, A., Credi, A., Astumian, R. D. & Ragazzon, G. Analysis of kinetic asymmetry in a multi-cycle reaction network establishes the principles for autonomous compartmentalized molecular ratchets. Chem 10, 3644–3655 (2024).
- Schormann, N., Ricciardi, R. & Chattopadhyay, D. Uracil-DNA glycosylases—structural and functional perspectives on an essential family of DNA repair enzymes. *Protein Sci.* 23, 1667–1685 (2014).

- 44. Hall-Thomsen, H. et al. Directing uphill strand displacement with an engineered superhelicase. ACS Synth. Biol. 12, 3424–3432 (2023).
- 45. Zhang, D. Y. & Winfree, E. Control of DNA strand displacement kinetics using toehold exchange. *J. Am. Chem.* Soc. **131**, 17303–17314 (2009).
- 46. Mayer, T., Oesinghaus, L. & Simmel, F. C. Toehold-mediated strand displacement in random sequence pools. *J. Am. Chem. Soc.* **145**, 634–644 (2023).
- 47. Del Grosso, E. et al. Dissipative control over the toehold-mediated DNA strand displacement reaction. *Angew. Chem. Int. Ed.* **61**, e202201929 (2022).
- 48. Binks, L. et al. The role of kinetic asymmetry and power strokes in an information ratchet. *Chem* **9**, 2902–2917 (2023).
- 49. Aprahamian, I. & Goldup, S. M. Non-equilibrium steady states in catalysis, molecular motors, and supramolecular materials: why networks and language matter. *J. Am. Chem. Soc.* **145**, 14169–14183 (2023).
- 50. Marchetti, T., Roberts, B. M. W., Frezzato, D. & Prins, L. J. A minimalistic covalent bond-forming chemical reaction cycle that consumes adenosine diphosphate. *Angew. Chem. Int. Ed.* **63**, e202402965 (2024).
- 51. Liu, H.-K. et al. Structural influence of the chemical fueling system on a catalysis-driven rotary molecular motor. *J. Am. Chem. Soc.* **147**, 8785–8795 (2025).
- 52. Penocchio, E., Rao, R. & Esposito, M. Thermodynamic efficiency in dissipative chemistry. *Nat. Commun.* **10**, 3865 (2019).
- 53. Kar, H., Goldin, L., Frezzato, D. & Prins, L. J. Local self-assembly of dissipative structures sustained by substrate diffusion. *Angew. Chem. Int. Ed.* **63**, e202404583 (2024).
- 54. Sorrenti, A., Leira-Iglesias, J., Sato, A. & Hermans, T. M. Non-equilibrium steady states in supramolecular polymerization. *Nat. Commun.* **8**, 15899 (2017).
- Brown, A. I. & Sivak, D. A. Theory of nonequilibrium free energy transduction by molecular machines. *Chem. Rev.* 120, 434–459 (2020).
- Shannon, C. E. A mathematical theory of communication. *Bell Syst. Tech. J.* 27, 379–423 (1948).
- 57. Hartich, D., Barato, A. C. & Seifert, U. Nonequilibrium sensing and its analogy to kinetic proofreading. *New J. Phys.* **17**, 055026 (2015).
- Ivanov, N. M., Baltussen, M. G., Fernández Regueiro, C. L., Derks, M. T. G. M. & Huck, W. T. S. Computing arithmetic functions using immobilised enzymatic reaction networks. *Angew. Chem. Int. Ed.* 62, e202215759 (2023).
- 59. Ehrich, J. & Sivak, D. A. Energy and information flows in autonomous systems. *Front. Phys.* **11**, 1108357 (2023).
- Kriebisch, C. M. E. et al. Template-based copying in chemically fuelled dynamic combinatorial libraries. *Nat. Chem.* 16, 1240–1249 (2024).
- Stasi, M. et al. Regulating DNA-hybridization using a chemically fueled reaction cycle. J. Am. Chem. Soc. 144, 21939–21947 (2022).

Publisher's note Springer Nature remains neutral with regard to jurisdictional claims in published maps and institutional affiliations.

Springer Nature or its licensor (e.g. a society or other partner) holds exclusive rights to this article under a publishing agreement with the author(s) or other rightsholder(s); author self-archiving of the accepted manuscript version of this article is solely governed by the terms of such publishing agreement and applicable law.

© The Author(s), under exclusive licence to Springer Nature Limited 2025

Methods

Quantifying selectivity with Shannon entropy

In this analysis, with input **T**, the red fluorescence marks a 'correct' output, whereas green fluorescence marks an 'incorrect' output. The probability of a correct output, where **T** binds **R**, is given by the proportion of fluorescent duplexes with red fluorescence, p(red) = [RT]/([RT] + [GT]). For any value of p(red) < 1, uncertainty in the fluorescence outcome of molecular recognition is introduced.

In information theory, the uncertainty associated with the measurement of a random variable (fluorescence output) is quantified by Shannon entropy^{21,56}:

$$H = \sum_{n} -p(n) \log_{2}[p(n)]$$

$$= -p(\text{red}) \log_{2}[p(\text{red})] - p(\text{green}) \log_{2}[p(\text{green})].$$
(1)

Units of \log_2 are chosen to convey Shannon entropy and, hence, uncertainty reduction in units of bits. Shannon entropy (equation (1)) is a non-negative quantity with a maximum value of $H_{\max}=1$ (for normalized probability distributions) corresponding to unbiased duplex formation, p(red)=p(green)=0.5. In such a scenario, one has no information on the fluorescence output as the fluorescence colour of a random duplex would be unbiased. For non-uniform probability distributions, that is, when molecular recognition favours the desired output, (that is where p(red)>p(green)), $H<H_{\max}$, leading to reduced uncertainty associated with the fluorescence output. Such a reduction can be interpreted as a measure of the amount of information (I) learnt by reading the output.

$$I = H_{\text{max}} - H = 1 + p \text{ (red) } \log_2[p \text{ (red)}] + p \text{ (green) } \log_2[p \text{ (green)}].$$
 (2)

In the case of perfect selectivity in molecular recognition, p(red) = 1, H = 0 and I = 1. As the colour of the fluorescence output is a binary variable, the maximum amount of information in this case is 1 bit.

In this work, we are interested in a quantitative estimate of the selectivity in terms of uncertainty reduction enabled by the information ratchet mechanism that we implemented to bias molecular recognition (Fig. 4c-e(iii)) relative to an unbiased pre-sorted state (Fig. 4c-e(i)) and equilibrium sorted state (Fig. 4c-e(i)). Therefore, equation (2) was used to quantify selectivity in terms of Shannon entropy reduction (Fig. 4d). Furthermore, equation (2) allows the quantification of Shannon entropy reduction for any given selectivity ([RT]/[GT]; Supplementary Fig. 26).

In Supplementary Section 6.3, we demonstrate that in the context where the input is also a binary variable, the ability of an information ratchet to reduce the Shannon entropy of the molecular recognition

output is directly related to signal transduction accuracy in terms of mutual information. between the input and output.

Data availability

All data and materials are available from the corresponding authors upon reasonable request.

References

62. Cover, T. M. & Thomas, J. A. Elements of Information Theory Vol. 2012 (John Wiley & Sons, 2012).

Acknowledgements

This work was financially supported by the Italian Ministry of Education and Research (grant nos. 2022TSB8P7 and P2022ANCEK to L.J.P. and F.R.), European Research Council (ERC; 819160 to F.R.), Associazione Italiana per la Ricerca sul Cancro (AIRC; project no. 21965 to F.R). This work has been supported by 'PNRR M4C2-Investimento 1.4- CN0000041' financed by NextGenerationEU (to F.R. and E.D.G.). We thank S. Borsley for helpful discussions.

Author contributions

L.J.P. and F.R. conceptualized and designed the project and supervised the work. E.D.G. performed the measurements and design optimization. B.M.W.R. processed and interpreted the data and performed the kinetic analysis. B.M.W.R. and E.P. performed the thermodynamic analysis. B.M.W.R., L.J.P. and E.P. drafted the manuscript with feedback from E.D.G. and F.R.

Competing interests

The authors declare no competing interests.

Additional information

Supplementary information The online version contains supplementary material available at https://doi.org/10.1038/s41565-025-01982-5.

Correspondence and requests for materials should be addressed to Francesco Ricci or Leonard J. Prins.

Peer review information *Nature Nanotechnology* thanks Byunghwa Kang, Thomas Ouldridge and the other, anonymous, reviewer(s) for their contribution to the peer review of this work.

Reprints and permissions information is available at www.nature.com/reprints.